Novel agent #2714 potently inhibits lung cancer growth by suppressing cell proliferation and by inducing apoptosis *in vitro* and *in vivo*

WENJIE LU[1*], QIANQIAN SUN[1*], BO CHEN[2], YAN LI[3], YOUZHI XU[1] and SIYING WANG[1]

[1]School of Basic Medicine, Anhui Medical University, Hefei, Anhui 230032;
[2]Department of Gastrointestinal Surgery, The First Affiliated Hospital of Anhui Medical University, Hefei, Anhui 230022;
[3]Pharmacodynamics Pharmacokinetics Early Safety Evaluation Model Animals, Cancer Center,
West China Hospital, Sichuan University, Chengdu, Sichuan 610041, P.R. China

Abstract. The use of small molecule compounds to inhibit cell proliferation is one of the most promising approaches in cancer therapy. In the present study, a cell viability assay, flow cytometry analysis, western blotting and mouse xenograft models were used to investigate the anticancer activities of #2714 and its underlying mechanisms in lung cancer. The present *in vitro* results suggested that #2714 significantly inhibited the viability of the human non-small cell lung cancer line SPC-A1 in a concentration- and time-dependent manner, with a half-maximal inhibitory concentration value of 5.54 μM after 48 h of treatment. Additionally, #2714 inhibited SPC-A1 cell proliferation via the Wnt/β-catenin pathway and by impairing mitochondrial membrane potential. The protein expression levels of Wnt 3a, Wnt 5a/b, phosphorylated (p)-β-catenin, p-glycogen synthase kinase 3β, and p-mitogen-activated protein kinase 14 were downregulated following treatment with #2714. Furthermore, using a mouse xenograft model, #2714 was identified to significantly inhibit tumor growth and to decrease cancer cell proliferation *in vivo*. #2714 may represent a novel effective anticancer compound targeting lung cancer cells. Additionally, #2714 was able to induce apoptosis and decrease cell proliferation in SPC-A1 cells via the Wnt/β-catenin pathway.

Correspondence to: Dr Youzhi Xu or Professor Siying Wang, School of Basic Medicine, Anhui Medical University, 81 Mei Shan Road, Hefei, Anhui 230032, P.R. China
E-mail: xuyouzhi@ahmu.edu.cn
E-mail: sywang@ahmu.edu.cn

*Contributed equally

Introduction

Lung cancer is the leading type of cancer in terms of incidence and mortality worldwide (1,2). Cytotoxic chemotherapy drugs represent the principal clinical option for lung cancer therapy. However, the 1-year and 5-year survival rates are <5% in certain Asian countries and regions (1,3,4). Additionally, chemotherapy drugs are associated with toxicity and multiple side effects (5). Targeted molecular therapy using small molecule drugs is a promising novel approach that may be used in the future to treat patients with lung cancer. Previous studies demonstrated the efficacy of targeted therapy against lung cancer in preclinical and clinical trials (5,6). Previous studies identified the effects of novel anticancer compounds on lung cancer cells (7-11), and inhibitors of the phosphatidylinositol 3-kinase/AKT serine/threonine kinase 1 (AKT; LY294002) and mitogen-activated protein kinase (MAPK; PD98059) signaling pathways were used to examine the role of caspases, AKT and/or MAPK in the apoptosis-inducing activity of the compounds identified (8,9). Additionally, lung cancer cell lines such as A549 cells and HepG2 liver cancer cells have been previously used to perform pharmacodynamic screenings (7,8).

Various novel compounds have been identified as promising agents in the treatment of lung cancer, and a number of these drugs were able to effectively suppress cell proliferation and metastasis in lung cancer (12). However, various drugs are associated with multiple side effects, moderate response rates and drug resistance (13,14). Therefore, the identification of novel compounds exhibiting increased effectiveness and safety, and the improvement of targeted lung cancer therapies, are urgently required.

The Wnt signaling pathway and its downstream factors serve an important role in carcinogenesis and may regulate cancer progression by influencing various processes, including cancer growth, metastasis and cell apoptosis (15). A previous study demonstrated that the Wnt/β-catenin pathway may regulate oncogenesis in various types of cancer, and hyperactivity of the Wnt/β-catenin pathway was identified to promote carcinogenesis (16). The Wnt/β-catenin pathway

regulates the proteosomal degradation of β-catenin via the β-catenin destruction complex, consisting of APC regulator of WNT signaling pathway, axin 1/2 and glycogen synthase kinase 3β (GSK-3β) (17). Therefore, the Wnt signaling pathway is involved in regulating the cytoplasmic levels of β-catenin. Extracellular Wnt ligands are able to bind to the frizzled receptors, transducing the signal to the intracellular protein dishevelled, thus inhibiting the β-catenin destruction complex and promoting the nuclear translocation of β-catenin. In the nucleus, β-catenin is able to induce the transcription of Wnt ligands and multiple downstream effector genes (18,19).

The activation of the Wnt/β-catenin pathway, which may lead to the upregulation of certain Wnt ligands, was identified in ~50% of all cases of non-small cell lung cancer (NSCLC) and primary lung cancer (20). Additionally, a previous study demonstrated that the downregulation of the Wnt signaling pathway was able to suppress cell proliferation in NSCLC (20). Therefore, Wnt may represent a promising therapeutic target for NSCLC.

Apoptosis is a programmed cell death process regulated by various cellular signals (21-25). The induction of apoptosis is a promising approach in cancer therapy, and various novel clinical chemotherapeutic strategies have been developed, with the aim of increasing apoptosis sensitivity by activating certain signaling pathways in cancer cells (26). Furthermore, cell proliferation serves an important role in the expansion of solid tumors, and the inhibition of proliferation may prevent cancer growth and metastasis (27). Our previous studies identified novel small molecular compounds with anticancer properties in preclinical models that may be used in targeted therapies to treat cancer (7,28,29). These compounds were identified to inhibit angiogenesis and cell proliferation, and to promote apoptosis and autophagy, thus exhibiting anticancer activity.

The aim of the present study was to investigate the anticancer properties and the mechanisms of action of #2714, a molecule identified in our previous study (7). The present study focused on the therapeutic potential of #2714 in lung cancer. In particular, the effects of #2714 on cancer cell proliferation and its ability to influence the Wnt/β-catenin and mitochondria-mediated apoptotic pathways were investigated.

Materials and methods

Preparation of #2714. In the present study, the pharmacological activity of #2714 was investigated. The chemical structure of #2714 was presented in our previous study (7). #2714 was one of the candidate compounds identified in our previous study investigating the targets of YL4073 (8). A computer-aided drug design method was used to examine the molecular docking of #2714 (7,8,26,29). The results suggested that #2714 may be associated with cell apoptosis and proliferation. Following drug design, #2714 was synthesized in our laboratory (7). To perform the *in vitro* experiments, #2714 was dissolved in dimethyl sulfoxide (Sigma-Aldrich; Merck KGaA, Darmstadt, Germany) and stored at 4°C. #2714 was diluted in culture medium to a final concentration of 0.1% (v/v) and cells were treated with various concentrations of #2714 (0-20 μM). For the *in vivo* experiments, #2714 was resuspended in 1.0% sodium carboxymethyl cellulose (Sigma-Aldrich; Merck KGaA) for a final concentration of 10 mg/ml, and was administered daily to each animal by gavage at various concentrations (25-100 mg/kg/day) at volumes of 10 ml/kg/day.

Materials. The Cell Counting Kit-8 (CCK-8) was purchased from Dojindo Molecular Technologies, Inc. (Kumamoto, Japan). The 5-ethynyl-2-deoxyuridine (EdU) proliferation assay kit was purchased from Guangzhou RiboBio Co., Ltd. (Guangzhou, China). Anti-marker of proliferation Ki-67 (MKI67, 1:50 dilution, cat. no. 550609) and Matrigel were purchased from BD Biosciences (San Jose, CA, USA). The primary antibodies Wnt3a (cat. no. ab28472) were obtained from Abcam Company (Cambridge, MA, USA), the primary antibodies Wnt5a/b (cat. no. 2530), t-β-catenin (cat. no. 9562), p-β-catenin (cat. no. 2009), t-GSK-3β (cat. no. 12456), p-GSK-3β (cat. no. 9336), t-p38 (MAPK14, cat. no. 9212); p-MAPK14 (cat. no. 4511), β-actin (cat. no. 4967) and horse-radish peroxidase (HRP)-conjugated secondary antibodies (cat. nos. 7074 and 7076) were obtained from Cell Signaling Technology, Inc. (Danvers, MA, USA). All the chemicals used in the present study were of analytical grade (30).

Cell culture. The human NSCLC cell line SPC-A1 and human 293 cells were purchased from the American Type Culture Collection (Manassas, VA, USA). SPC-A1 cells were cultured in RPMI-1640 medium and 293 cells were cultured in Dulbecco's modified Eagle's medium (both from Thermo Fisher Scientific, Inc., Waltham, MA, USA); media were supplemented with 10% fetal bovine serum (FBS; Gibco; Thermo Fisher Scientific, Inc.), 2 mM glutamine and 1% antibiotic-antimycotic solution at 37°C with 5% CO_2.

Animals. A total of 108 female BALB/c nude mice (age, 6-8 weeks; weight, 18-22 g) were purchased from Beijing Animal Center (Beijing, China), and maintained under controlled specific pathogen-free experimental conditions at 21°C with 55% humidity under a 12:12-h light/dark cycle, with free access to food and water. For *in vivo* experiment, when tumor size reached ~1,500 mm^3, animals were sacrificed, and tumor tissues were harvested. All animal experiments were performed in compliance with the ARRIVE guidelines and the Guide for the Care and Use of Laboratory Animals (31). Animal experiments were approved by The Experimental Animal Ethics Committee of Anhui Medical University (Hefei, China).

Cell proliferation assay. Cell proliferation was examined by CCK-8 assay following treatment with #2714. In total, 3-5x10^3 cells were seeded in 96-well plates in triplicate at 37°C with 5% CO_2 for 24 h. The 293 cells were treated with #2714 (0-20 μM) at 37°C for 48 h, whereas SPC-A1 cells were treated at 37°C for 6-72 h. Subsequently, 100 μl culture medium containing 10 μl CCK-8 solution was added to the wells and incubated at 37°C for 2-4 h in the dark. The absorbance values were measured using a Spectra MAX M5 microplate spectrophotometer (Molecular Devices, LLC, Sunnyvale, CA, USA) at 450 nm. The inhibitory rate was calculated as previously described (7). Subsequently, the half-maximal inhibitory concentration (IC$_{50}$) values of #2714 were determined by using GraphPad Prism 7.0 Software (GraphPad Software, Inc., La Jolla, CA, USA).

Flow cytometry analysis. Flow cytometry (FCM) was used to analyze cell apoptosis and mitochondrial membrane potential ($\Delta\Psi m$) by staining the cells with propidium iodide (PI) and rhodamine-123 (Rho 123) (both from Sigma-Aldrich; Merck KGaA), respectively. In total, $1x10^5$ SPC-A1 cells were cultured in 6-well plates for 24 h. Following treatment with #2714 for 48 h, SPC-A1 cells were incubated with 50 μl/ml PI solution, 0.1% Triton X-100 and 0.1% sodium citrate, or 5 μg/ml Rho 123 at 37°C with 5% CO_2 for 30 min in darkness. PI-stained and Rho 123-stained cells were analyzed using a flow cytometer (FACS Verse; BD Biosciences). Data were analyzed using FlowJo software Version 7.6 (FlowJo LLC, Ashland, OR, USA).

EdU assay. In total, $1x10^5$ SPC-A1 cells were cultured on coverslips in triplicate in 24-well plates and treated with 0, 2.5, 5 or 10 μM #2714 for 48 h as aforementioned. Cell proliferation was determined using an EdU incorporation assay kit, in which Hoechst 33342 was included (Guangzhou RiboBio Co., Ltd.) according to the manufacturer's protocol. Briefly, following treatment with #2714, cells were incubated with 500 μl EdU solution (50 μM) diluted with completed medium at 37°C in darkness for 2 h, then fixed with 4% paraformaldehyde at room temperature for 30 min and stained with 500 μl Hoechst 33342 solution at room temperature in darkness for a further 30 min. The percentage of proliferating cells was determined using an inverted fluorescence microscope (magnification, x40; Zeiss AG, Oberkochen, Germany).

Matrigel invasion assay. Transwell filter inserts (EMD Millipore, Billerica, MA, USA) were precoated with Matrigel (BD Biosciences) for 30 min at 37°C. RPMI-1640 with 10% FBS was plated in the lower chamber, and $4x10^4$ cells were seeded in the upper chamber in serum-free RPMI-1640 medium. Various concentrations of #2714 were placed in the upper chambers (0-10 μM), and plates were incubated for 24 h at 37°C with 5% CO_2. Subsequently, 0.1% crystal violet was used to stain the cells that had migrated from the upper chamber to the lower chamber for 4 h at 37°C. Cells were visualized using a fluorescence microscope equipped with a digital camera (magnification, x40; Olympus Corporation, Tokyo, Japan). Cells were counted, and the results are presented as the percentage of invasive cells in the treatment group compared with the control (28).

Western blot analysis. Western blot analysis was performed to investigate the mechanisms underlying #2714 function, according to previous studies (7,8). Cells were lysed in radioimmunoprecipitation buffer (1% NP-40, 0.5% deoxycholate, 0.2% SDS, 150 mM sodium chloride, 50 mM Tris-HCl, pH 7.4) containing 0.1% phenylmethane sulfonyl fluoride and 1% proteinase inhibitor cocktail (Sigma-Aldrich; Merck KGaA). Protein concentration was measured using the Bio-Rad protein assay kit (Bio-Rad Laboratories, Inc., Hercules, CA, USA). The lysates were loaded with 5X SDS sample buffer and denatured, then proteins (20 μg/lane) were subjected to 6-12% SDS-PAGE and subsequently transferred onto polyvinylidene difluoride membranes. Then, the membranes were blocked for 1 h in 5% dried milk in TBS-0.1% Tween-20 at room temperature, and the protein expression levels of factors associated with the Wnt/β-catenin pathway, apoptosis and proliferation were detected in SPC-A1 cells with the primary antibodies overnight at 4°C (1:500 for Wnt3a, and 1:1,000 for Wnt5a/b, t-/p-β-catenin, t-/p-GSK-3β, t-/p-MAPK14 and β-actin), prior to incubation with HRP-conjugated secondary antibodies for 2 h at 37°C (1:5,000-8,000). The protein bands were visualized using Amersham enhanced chemiluminescence reagent (GE Healthcare Life Sciences, Shanghai, China). Densitometric analysis was performed using Quantity One 1-D analysis software Version 4.6.6 (Bio-Rad Laboratories, Inc.). β-actin was used as the loading control.

Tumorigenesis in vivo. In total, $5x10^6$ SPC-A1 cells were subcutaneously injected into the right side of the back of female BALB/c nude mice. The tumor volumes were measured every other day, and mice carrying a tumor of 100-300 mm^3 in volume were randomly divided into four groups (n=5 in each group). Subsequently, #2714 was administered by gavage at various concentrations (0, 25, 50 and 100 mg/kg/day) every day. The clinical symptoms of NSCLC were observed daily. After 18 days, mice were sacrificed with CO_2 (air displacement rate, 20%/min), and tumor tissues were removed, weighed and their volumes were calculated. A bilateral Vernier caliper was used to measure the tumor length (long diameter) and width (short diameter) every three days. The tumor volume was calculated as: Tumor volume (mm^3)=0.5 x length (mm) x width^2 (mm) (32).

Immunohistochemical (IHC) analysis in vivo. IHC analysis was performed on 4% paraformaldehyde-fixed (4°C for 3-7 days) paraffin-embedded tumor tissues from the mice injected with SPC-A1 cells and treated with #2714 at a concentration of 100 mg/kg/day for 14 days (n=8 in each group). MKI67 staining of 4-μm sections was performed to the detect malignant features of the tumors, as previously described (33). Briefly, the sections were heated at 65°C for 2 h, deparaffinized and rehydrated with xylene and a graded ethanol series (100, 95, 80 and 50%). Then, the sections were heated for 10 min at ~100°C in citrate buffer (10 mM citric acid, 0.05% Tween-20, pH 7.4) using a pressure cooker, followed by cooling for antigen retrieval. To block endogenous peroxidase activity, the sections were immersed in 0.3% H_2O_2 for 10 min at room temperature, and washed in distilled water. Then, the sections were incubated with 3% FBS (Gibco; Thermo Fisher Scientific, Inc.) at 37°C for 30 min to block non-specific binding of immunoglobulin. Sections were subsequently incubated with primary antibody MKI67 (1:50) overnight at 4°C, washed with PBS three times for 5 min, and then incubated with HRP-conjugated anti-mouse IgG (1:5,000; cat. no. 7076) for 20 min at 37°C. Sections were then reacted with 3,3'-diaminobenzidine solution (1:200; ZSGB-BIO; OriGene Technologies, Inc., Beijing, China) for 2 min at room temperature, following which the reaction was stopped with dH_2O, and sections were counterstained with hematoxylin for 1 min at room temperature. Finally, sections were washed with dH_2O, dehydrated in a graded ethanol series (50, 75 and 100%) and incubated in xylene prior to mounting. Sections were observed under a light microscope (magnification, x200; Zeiss AG); three equal-sized fields per slide were analyzed.
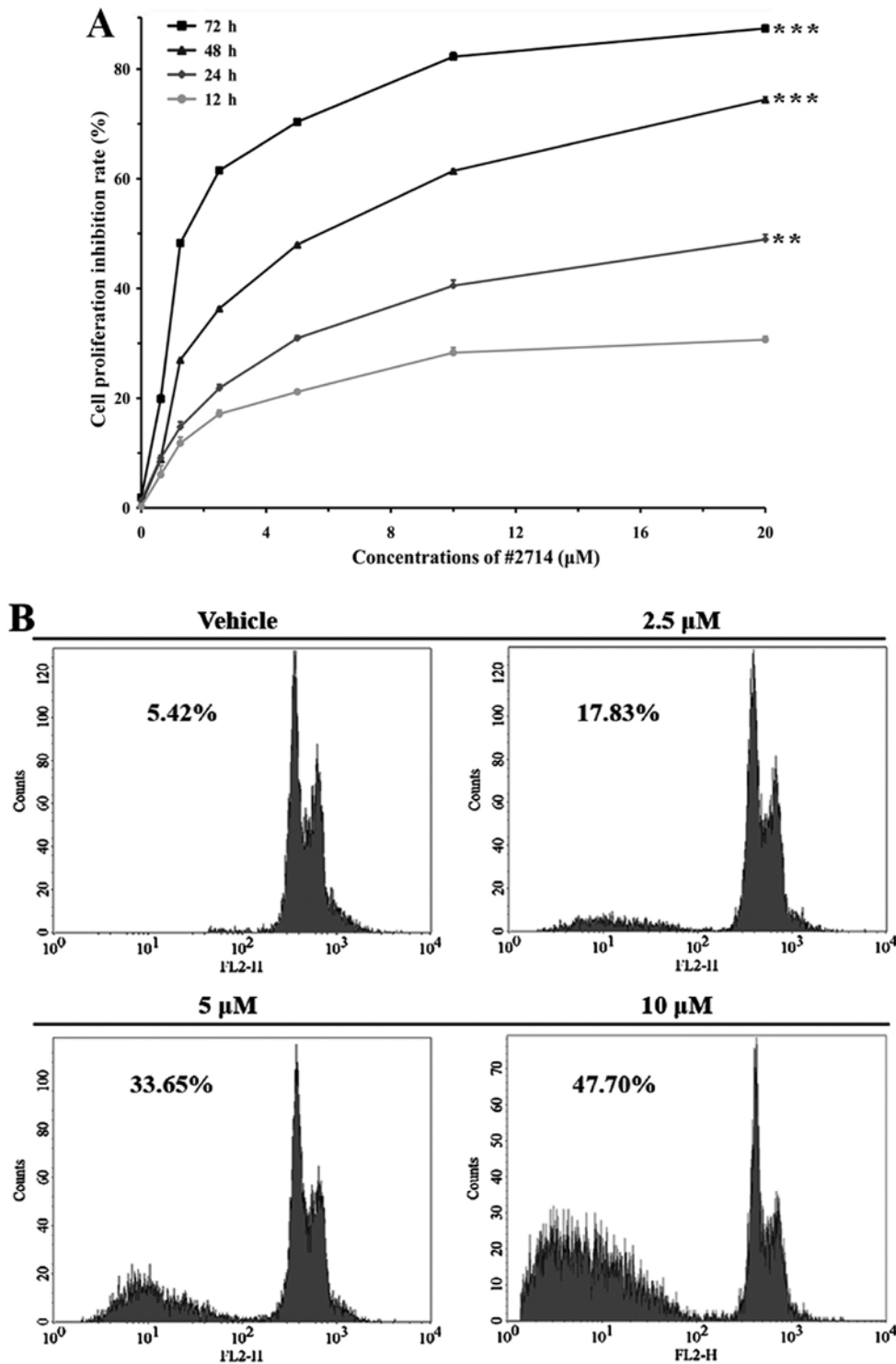
Figure 1. Treatment with #2714 inhibits proliferation and induces apoptosis *in vitro*. (A) A Cell Counting Kit-8 assay was performed to detect the inhibitory effects of #2714 on SPC-A1 cells. (B) Apoptosis rates were detected by flow cytometry following treatment with #2714 for 48 h. n=3 in each group. [**]$P<0.01$, [***]$P<0.001$ vs. vehicle group.

H&E staining was performed to investigate the morphology of heart, liver, spleen, lung and kidney tissue following treatment with #2714. Briefly, following collection and fixed with 4% paraformaldehyde (4°C for 3-7 days), paraffin-embedded tissues were sectioned (4 um), deparaffinized, rehydrated and stained at room temperature with hematoxylin for 3-5 sec and eosin (both from Poly Scientific R&D Corp., Bayshore, NY, USA) for 20-30 sec. Sections were observed under a light

microscope (magnification, x100; Zeiss AG); three equal-sized fields per slide were analyzed.

Statistical analysis. Data are presented as the mean ± standard deviation or standard error of the mean of three experiments. SPSS software (version 13.0; SPSS, Inc., Chicago, IL, USA) was used to perform statistical analysis. Student's t-test or one-way analysis of variance followed by Dunnett's t-test was
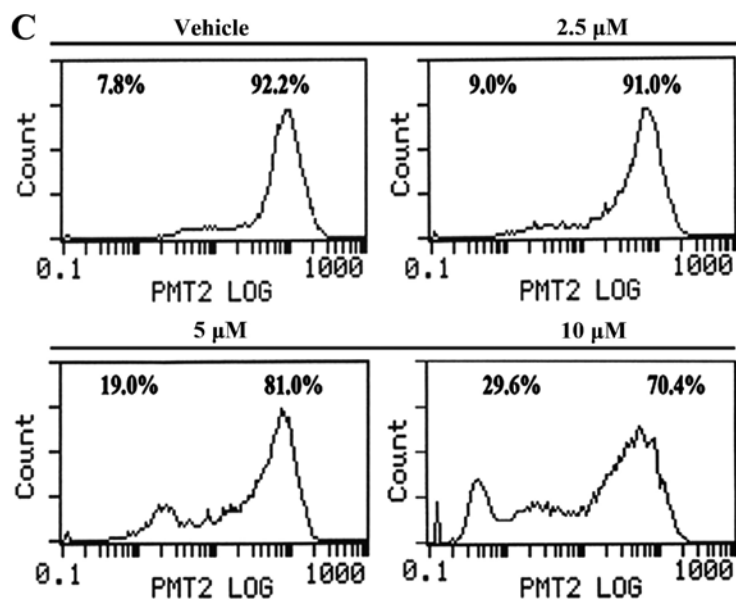
Figure 1. Continued. (C) Treatment with #2714 for 48 h impaired the mitochondrial membrane potential, as assessed by Rhodamine 123 staining. Data are presented as the mean ± standard error of the mean.

used to analyze the differences between groups. $P<0.05$ was considered to indicate a statistically significant difference.

Results

Effects of #2714 on tumor cell proliferation in vitro. A CCK-8 assay was used to detect the proliferation of cancerous and non-cancerous cells following treatment with #2714 or vehicle for 48 h. Subsequently, the IC_{50} values of #2714 were determined. The present results suggested that #2714 decreased tumor cell proliferation. The IC_{50} in the NSCLC cell line SPC-A1 was 5.54 μM after 48 h (Fig. 1A). Furthermore, #2714 exhibited a favorable safety profile in the non-cancerous embryonic human cell line 293 (data not shown). Furthermore, the present CCK-8 results suggested that #2714 inhibited the proliferation of SPC-A1 cells in a time- and concentration-dependent manner. The IC_{50} values of #2714 were 18.8 and 1.91 μM after 24 and 72 h of treatment, respectively.

Treatment with #2714 induces apoptosis and inhibits proliferation in vitro. Treatment with #2714 for 48 h markedly induced apoptosis in SPC-A1 cells. The FCM results suggested that the percentage of apoptotic cells following treatment with #2714 increased in a concentration-dependent manner. The percentage of apoptotic cells following a 48-h treatment with #2714 at 2.5 μM was 17.83% and it increased to 47.70% at 10 μM (Fig. 1B). Furthermore, the effects of #2714 on $\Delta\Psi$m were assessed by measuring the intensity of Rho 123 (Fig. 1C). The percentage of Rho 123-positive cells was 92.2% in the vehicle group; however, it decreased to 70.4% following a 48 h treatment with #2714 at 10 μM. The present results suggested that the permeability of the mitochondrial membrane and $\Delta\Psi$m were severely impaired following treatment with #2714. The EdU assay results suggested that treatment with #2714 inhibited SPC-A1 cell proliferation in a concentration-dependent manner (Fig. 2A). Additionally, the invasive ability of SPC-A1 cells was decreased following treatment with #2714

and the percentage of invasive cells was inversely proportional to the concentration of #2714 (Fig. 2B). The EdU assay results suggested that the percentage of cells in the S phase decreased by 20.2-68.08% in a concentration-dependent manner following treatment with 2.5-10 μM (Fig. 2C). Additionally, the invasion assay results suggested that the percentage of invasive SPC-A1 cells decreased by 21.08-63.70% depending on the concentration of #2714 (Fig. 2D).

Effects of #2714 on the Wnt/β-catenin signaling pathway in vitro. Western blotting was used to investigate the mechanism underlying the function of #2714. The protein expression levels of Wnt3a, Wnt5a/b and p-β-catenin were markedly downregulated following treatment with #2714 compared with vehicle group; however, there was no significant difference in expression following treatment with 10 μM compared with 5 μM #2714 (Fig. 3A). Furthermore, treatment with #2714 at 10 μM significantly downregulated the ratios of p-MAPK14 to total (t-)MAPK14 and of p-GSK-3β to t-GSK-3β in a concentration-dependent manner in SPC-A1 cells, compared with treatment at 5 μM (Fig. 3B).

Antitumor activity and safety evaluation of #2714 in vivo. To determine the antitumor effects of #2714 *in vivo*, SPC-A1 cells were subcutaneously injected into the right side of the back of mice to establish a xenograft tumor model. Treatment with #2714 at 100 mg/kg inhibited tumor growth by 68.56% compared with the vehicle after 18 days of treatment (Fig. 4A). Notably, body weight was not altered following treatment with #2714 (Fig. 4B). Furthermore, the tumor weights were significantly decreased following treatment with #2714 (Fig. 4C). In addition, IHC analysis suggested that the number of proliferating cells, as assessed by MKI67 staining, was markedly decreased in tumor tissues following treatment with #2714 at 100 mg/kg/day for 14 days (Fig. 4D). Additionally, H&E staining was conducted to investigate the morphology of the heart, liver, spleen, lungs and kidneys following treatment with
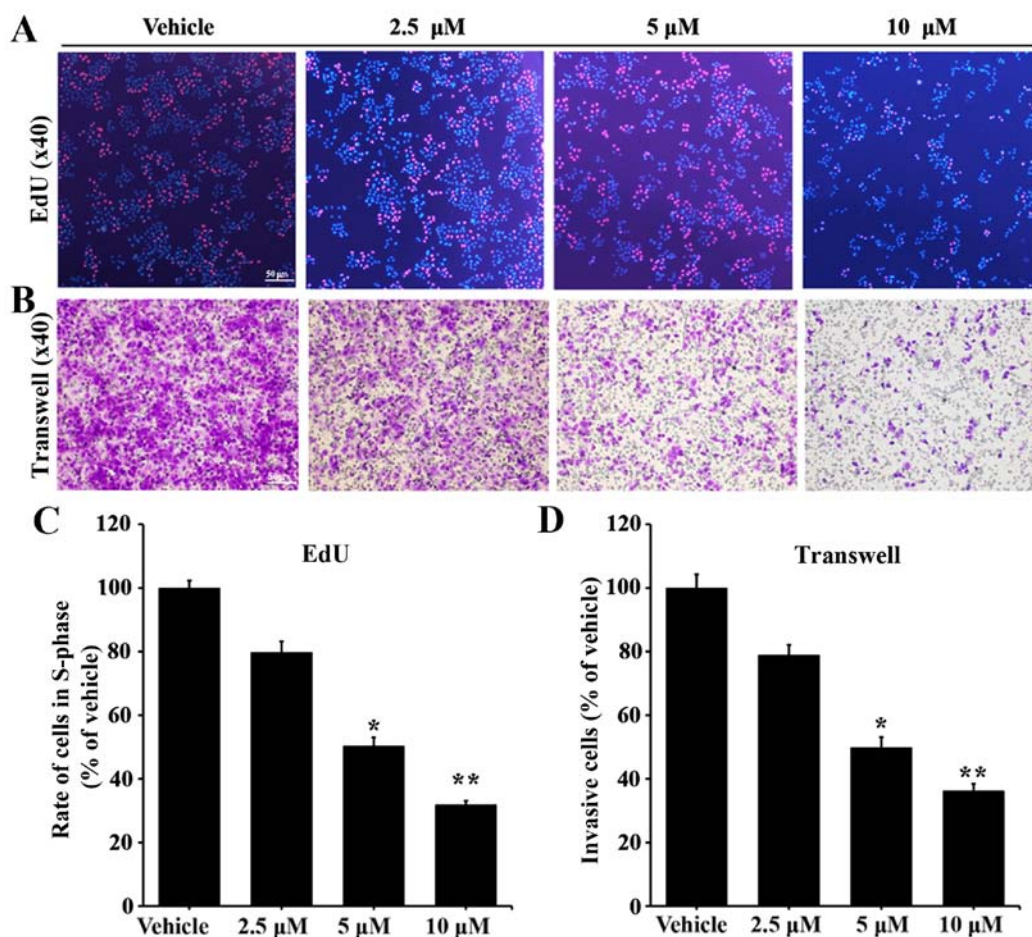
Figure 2. Treatment with #2714 inhibits the proliferation and invasion of SPC-A1 cells *in vitro*. (A) An EdU incorporation assay was used to assess the effects of #2714 on SPC-A1 cell proliferation after 48 h of treatment. The nuclei of SPC-A1 cells are stained in blue by Hoechst 33342 and in red by EdU. (B) SPC-A1 cell invasion following treatment with #2714 for 24 h, measured using Matrigel assays. (C) The percentage of S-phase cells, as assessed by EdU assay. (D) Percentage of invasive SPC-A1 cells as assessed using Matrigel assay. Data are presented as the mean ± standard error of the mean. Magnification, x40. *P<0.05, **P<0.01 vs. vehicle group. EdU, 5-ethynyl-2-deoxyuridine.

#2714; no abnormal or pathological alterations were detected (data not shown).

Discussion

NSCLC accounts for ~85% of all lung cancer cases worldwide. Lung cancer is the most common type of cancer and the leading cause of cancer-associated mortality worldwide (1). The 1-year and 5-year survival rates, and the progression-free survival rate remain poor. The Wnt signaling pathway was identified to be active in ~50% of human NSCLC cell lines and primary tumors (17). Notably, suppression of the activity of the Wnt signaling pathway may inhibit cell proliferation in human NSCLC (17). Therefore, the identification of novel compounds able to suppress the Wnt signaling pathway may facilitate the development of effective NSCLC targeted therapies. Previous studies have demonstrated that Wnt ligands and downstream effectors of the Wnt/β-catenin pathway may serve an important role in the regulation of tumor cell apoptosis and tumor metastasis (15,19,25). The Wnt/β-catenin pathway regulates the stability of β-catenin via its proteasomal degradation (19). Specifically, extracellular Wnt ligands are able to bind to the frizzled and LDL receptor related protein 5/6 receptors, transducing the signal to intracellular disheveled, leading to the

inhibition of the β-catenin destruction complex, thus inducing the translocation of β-catenin into the nucleus and the transcription of its target genes (34).

Decreased apoptotic and increased proliferation rates serve important roles in the pathogenesis, metastasis and chemoresistance of solid tumors (35). The use of chemically-synthesized small molecules to increase apoptosis sensitivity and inhibit proliferation of cancer cells is a promising and effective strategy to treat various types of cancer (36).

In the present study, the pharmacological activity of the novel compound #2714 was investigated. In previous studies investigating the therapeutic targets of YL4073 (7,8,28), #2714 was synthesized and identified as a promising candidate compound with anticancer properties (8,30). Additionally, in our previous studies, a computer-aided drug design method was used to investigate the molecular docking of #2714, and #2714 was predicted to be associated with cell apoptosis and proliferation (7,8,28). The present results suggested that #2714 significantly inhibited the proliferation of lung cancer cells via the Wnt/β-catenin signaling pathway, and induced cell apoptosis via the mitochondria-dependent pathway without affecting the functions of non-cancerous cells.

The *in vitro* CCK-8 experiments suggested that #2714 exhibited anticancer activities in lung cancer cells with a
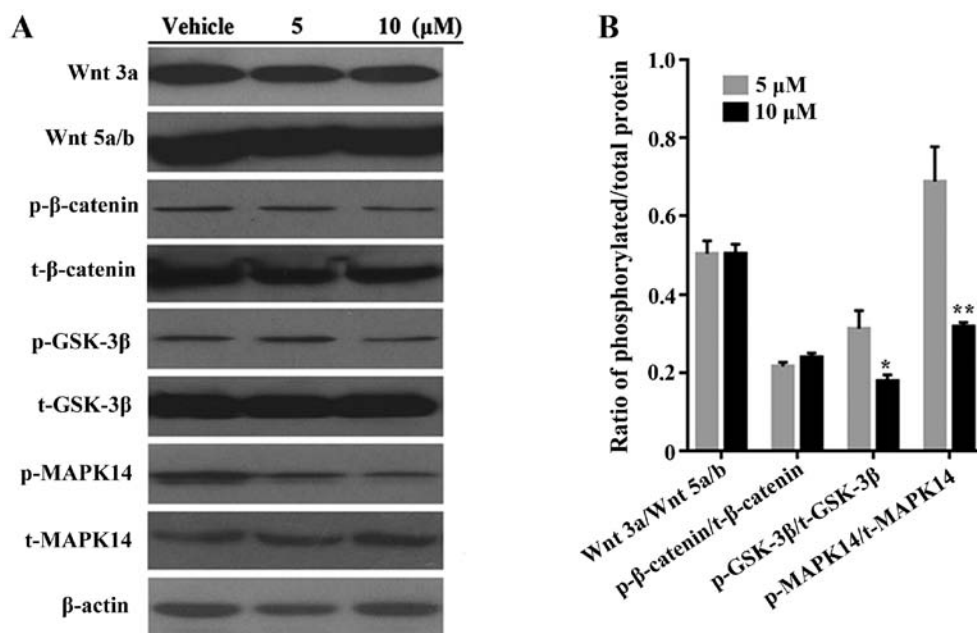
Figure 3. Effects of #2714 on the Wnt/β-catenin signaling pathway and proliferation-associated factors. SPC-A1 cells were treated with #2714 for 24 h at 5 and 10 μM. (A) Protein expression levels of Wnt3a, Wnt5a/b, t- and p-β-catenin, GSK-3β and p-MAPK14. (B) Quantification of western blotting results, as measured by densitometric analysis. Data are presented as the mean ± standard deviation. n=3 in each group. *P<0.05, **P<0.01 vs. respective 5 μM group. t-, total; p-, phosphorylated; MAPK14, mitogen activated protein kinase 14; GSK-3β, glycogen synthase kinase 3β.
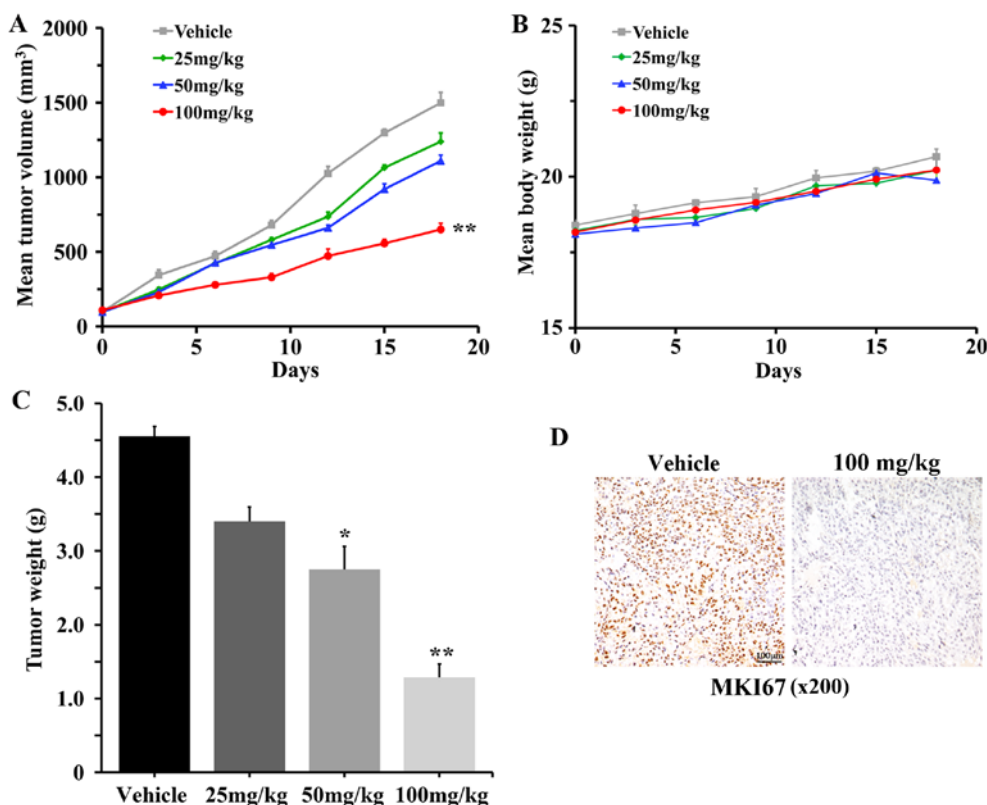

Figure 4. Anticancer activity of #2714 in vivo. BALB/c nude mice injected with SPC-A1 lung cancer cells were treated with #2714 at 0, 25, 50 and 100 mg/kg/day. (A) Tumor volumes and (B) body weights were measured every three days for 18 days. (C) Quantification of tumor weights following treatment with #2714 at various concentrations (n=5/group). (D) Immunohistochemical analysis of xenograft tumors was performed to investigate the protein expression level of MKI67 following treatment with #2714 at 100 mg/kg/day for 14 days (n=8/group). Magnification, x200. Data are presented as the mean ± standard error of the mean. *P<0.05, **P<0.01 vs. respective vehicle group. MKI67, marker of proliferation Ki-67.

low IC_{50} value. Notably, #2714 inhibited the proliferation of SPC-A1 cells in a concentration-dependent manner as

assessed by EdU assay, in line with the CCK-8 proliferation assay results. Furthermore, MAPK14 was previously identified

to be associated with the activity of various small molecular anticancer agents able to inhibit tumor cell proliferation and to promote apoptosis (37). In the present study, treatment with #2714 markedly downregulated the protein expression levels of components of the Wnt/β-catenin pathway. The present study aimed to investigate the effects of #2714 on tumor cell proliferation and on the protein expression level of p-MAPK14 in SPC-A1 cells. The present results suggested that #2714 inhibited cell proliferation by influencing the Wnt/β-catenin pathway in a time- and concentration-dependent manner.

Apoptosis induction is one of the most promising and effective strategies in cancer therapy (35). In the present study, #2714 was identified to be able to decrease the viability of SPC-A1 cells by inducing apoptosis, as assessed by FCM. Furthermore, the mechanism underlying apoptosis induction was investigated in the present study. Following treatment with #2714, SPC-A1 cells exhibited loss of ΔΨm. The impairment and loss of ΔΨm are important factors involved in the intrinsic apoptotic pathway (38). The present result suggested that the loss of ΔΨm may be associated with the anticancer effects of #2714.

In the present study, in order to investigate the pharmacodynamic activity and the mechanism of action of #2714, the antitumor activity of #2714 was examined using a mouse xenograft model *in vivo*. SPC-A1 cells were injected into mice, and tumor growth of mouse xenograft model were decreased by 68.56% following treatment with 100 mg/kg/day #2714. Furthermore, IHC analysis suggested that treatment with #2714 decreased the proliferation of cancer cells *in vivo*. Following treatment with #2714, mouse body weight was not altered, and abnormal pathological alterations were not observed, suggesting that #2714 may serve as an anticancer agent with a favorable safety profile.

In conclusion, the present study suggested that #2714 may represent a novel anticancer compound, exhibiting antiproliferative effects associated with the suppression of the Wnt/β-catenin and the mitochondria-mediated apoptosis pathways.

Availability of data and materials

The datasets used and/or analyzed during the current study are available from the corresponding author on reasonable request.

Authors' contributions

YX and SW conceived and designed the study. WL, QS and YX performed the experiments, collected and analyzed the data, and wrote the original drafts of manuscript. BC and YL made substantial contributions to the analysis and interpretation of data. WL, QS, BC, YL and YX revised the manuscript. All authors read and approved the final version of the manuscript.

Ethics approval and consent to participate

The animal experiments were performed in compliance with the ARRIVE guidelines and the Guide for the Care and Use of Laboratory Animals. The present study was approved by The Experimental Animal Ethics Committee of Anhui Medical University (Hefei, China).

Patient consent for publication

Not applicable.

Competing interests

The authors declare that they have no competing interests.

References

1. Siegel RL, Miller KD and Jemal A: Cancer statistics, 2017. CA Cancer J Clin 67: 7-30, 2017.
2. Blandin Knight S, Crosbie PA, Balata H, Chudziak J, Hussell T and Dive C: Progress and prospects of early detection in lung cancer. Open Biol 7: 170070, 2017.
3. Akamatsu H, Mori K, Naito T, Imai H, Ono A, Shukuya T, Taira T, Kenmotsu H, Murakami H, Endo M, et al: Progression-free survival at 2 years is a reliable surrogate marker for the 5-year survival rate in patients with locally advanced non-small cell lung cancer treated with chemoradiotherapy. BMC Cancer 14: 18, 2014.
4. Allemani C, Matsuda T, Di Carlo V, Harewood R, Matz M, Nikšić M, Bonaventure A, Valkov M, Johnson CJ, Estève J, et al: Global surveillance of trends in cancer survival 2000-14 (CONCORD-3): Analysis of individual records for 37 513 025 patients diagnosed with one of 18 cancers from 322 population-based registries in 71 countries. Lancet 391: 1023-1075, 2018.
5. Fennell DA, Summers Y, Cadranel J, Benepal T, Christoph DC, Lal R, Das M, Maxwell F, Visseren-Grul C and Ferry D: Cisplatin in the modern era: The backbone of first-line chemotherapy for non-small cell lung cancer. Cancer Treat Rev 44: 42-50, 2016.
6. Brückl W, Tufman A and Huber RM: Advanced non-small cell lung cancer (NSCLC) with activating EGFR mutations: First-line treatment with afatinib and other EGFR TKIs. Expert Rev Anticancer Ther 17: 143-155, 2017.
7. Lu WJ, Peng W, Sun QQ, Li YH, Chen B, Yu LT, Xu YZ, Wang SY and Zhao YL: #2714, a novel active inhibitor with potent arrested G2/M phase and antitumor efficacy in preclinical models. Cell Death Discov 4: 24, 2018.
8. Xu YZ, Zheng RL, Zhou Y, Peng F, Lin HJ, Bu Q, Mao YQ, Yu LT, Yang L and Yang SY: Small molecular anticancer agent SKLB703 induces apoptosis in human hepatocellular carcinoma cells via the mitochondrial apoptotic pathway in vitro and inhibits tumor growth in vivo. Cancer Lett 313: 44-53, 2011.
9. Xiao GH, Jeffers M, Bellacosa A, Mitsuuchi Y, Vande Woude GF and Testa JR: Anti-apoptotic signaling by hepatocyte growth factor/Met via the phosphatidylinositol 3-kinase/Akt and mitogen-activated protein kinase pathways. Proc Natl Acad Sci USA 98: 247-252, 2001.
10. Downward J: Use of RNA interference libraries to investigate oncogenic signalling in mammalian cells. Oncogene 23: 8376-8383, 2004.
11. Li P, Nijhawan D, Budihardjo I, Srinivasula SM, Ahmad M, Alnemri ES and Wang X: Cytochrome c and dATP-dependent formation of Apaf-1/caspase-9 complex initiates an apoptotic protease cascade. Cell 91: 479-489, 1997.
12. Printz C: Targeted therapy in lung cancer: Survival, quality of life improved for some patients. Cancer 120: 2625-2626, 2014.

13. Ramalingam SS, Blackhall F, Krzakowski M, Barrios CH, Park K, Bover I, Seog Heo D, Rosell R, Talbot DC, Frank R, *et al*: Randomized phase II study of dacomitinib (PF-00299804), an irreversible pan-human epidermal growth factor receptor inhibitor, versus erlotinib in patients with advanced non-small-cell lung cancer. J Clin Oncol 30: 3337-3344, 2012.
14. Hartmann JT, Haap M, Kopp HG and Lipp HP: Tyrosine kinase inhibitors-a review on pharmacology, metabolism and side effects. Curr Drug Metab 10: 470-481, 2009.
15. Anastas JN and Moon RT: WNT signalling pathways as therapeutic targets in cancer. Nat Rev Cancer 13: 11-26, 2012.
16. Brown K, Yang P, Salvador D, Kulikauskas R, Ruoholabaker H, Robitaille AM, Chien AJ, Moon RT and Sherwood V: WNT/β-catenin signaling regulates mitochondrial activity to alter the oncogenic potential of melanoma in a PTEN-dependent manner. Oncogene 36: 3119-3136, 2017.
17. Regmi SC, Park SY, Kim SJ, Banskota S, Shah S, Kim DH and Kim JA: The anti-tumor activity of Succinyl Macrolactin A is mediated through the β-catenin destruction complex via the suppression of tankyrase and PI3K/Akt. PLoS One 10: e0141753, 2015.
18. Zhan T, Rindtorff N and Boutros M: Wnt signaling in cancer. Oncogene 36: 1461-1473, 2018.
19. Clevers H and Nusse R: Wnt/β-catenin signaling and disease. Cell 149: 1192-1205, 2012.
20. Akiri G, Cherian MM, Vijayakumar S, Liu G, Bafico A and Aaronson SA: Wnt pathway aberrations including autocrine Wnt activation occur at high frequency in human non-small-cell lung carcinoma. Oncogene 28: 2163-2172, 2009.
21. Kreuzaler P and Watson CJ: Killing a cancer: What are the alternatives? Nat Rev Cancer 12: 411-424, 2012.
22. Shalini S, Dorstyn L, Dawar S and Kumar S: Old, new and emerging functions of caspases. Cell Death Differ 22: 526-539, 2015.
23. Pradelli LA, Bénéteau M and Ricci JE: Mitochondrial control of caspase-dependent and -independent cell death. Cell Mol Life Sci 67: 1589-1597, 2010.
24. Denisenko TV, Budkevich IN and Zhivotovsky B: Cell death-based treatment of lung adenocarcinoma. Cell Death Dis 9: 117, 2018.
25. Brentnall M, Rodriguez-Menocal L, De Guevara RL, Cepero E and Boise LH: Caspase-9, caspase- 3 and caspase-7 have distinct roles during intrinsic apoptosis. BMC Cell Biol 14: 32, 2013.
26. Azmi AS, Wang Z, Philip PA, Mohammad RM and Sarkar FH: Emerging Bcl-2 inhibitors for the treatment of cancer. Expert Opin Emerg Drugs 16: 59-70, 2011.
27. Wells A, Grahovac J, Wheeler S, Ma B and Lauffenburger D: Targeting tumor cell motility as a strategy against invasion and metastasis. Trends Pharmacol Sci 34: 283-289, 2013.
28. Xu YZ, Li YH, Lu WJ, Lu K, Wang CT, Li Y, Lin HJ, Kan LX, Yang SY, Wang SY and Zhao YL: YL4073 is a potent autophagy-stimulating antitumor agent in an *in vivo* model of Lewis lung carcinoma. Oncol Rep 35: 2081-2088, 2016.
29. Xu Y, Lu W, Yang P, Peng W, Wang C, Li M, Li Y, Li G, Meng N, Lin H, *et al*: A small molecular agent YL529 inhibits VEGF-D-induced lymphangiogenesis and metastasis in preclinical tumor models in addition to its known antitumor activities. BMC Cancer 15: 525, 2015.
30. Zheng RL, Zeng XX, He HY, He J, Yang SY, Yu YT and Yang L: Facile synthesis of 6-Aryl-3-cyanopyridine-2-(1H)-thiones from Aryl Ketones. J Synthetic Commun 42: 1521-1531, 2012.
31. Kilkenny C, Browne W, Cuthill IC, Emerson M and Altman DG; NC3Rs Reporting Guidelines Working Group: Animal research: Reporting in vivo experiments: The ARRIVE guidelines. J Physiol 160: 1577-1579, 2010.
32. Mitrofanova A, Aytes A, Zou M, Shen MM, Abate-Shen C and Califano A: Predicting drug response in human prostate cancer from preclinical analysis of in vivo mouse models. Cell Rep 12: 2060-2071, 2015.
33. Awazu Y, Nakamura K, Mizutani A, Kakoi Y, Iwata H, Yamasaki S, Miyamoto N, Imamura S, Miki H and Hori A: A novel inhibitor of c-Met and VEGF receptor tyrosine kinases with a broad spectrum of in vivo antitumor activities. Mol Cancer Ther 12: 913-924, 2013.
34. Niehrs C: The complex world of WNT receptor signalling. Nat Rev Mol Cell Biol 13: 767-779, 2012.
35. Villanueva MT: Targeted therapies: Priming apoptosis. Nat Rev Clin Oncol 10: 67, 2013.
36. Sarosiek KA, Fraser C, Muthalagu N, Bhola, PD, Chang WT, McBrayer SK, Cantlon A, Fisch S, Golomb-Mello G, Ryan JA, *et al*: Developmental regulation of mitochondrial apoptosis by c-Myc governs age- and tissue-specific sensitivity to cancer therapeutics. Cancer Cell 31: 142-156, 2017.
37. Fulda S: The PI3K/Akt/mTOR pathway as therapeutic target in neuroblastoma. Curr Cancer Drug Targets 9: 729-737, 2014.
38. Davidson SM, Lopaschuk GD, Spedding M and Beart PM: Mitochondrial pharmacology: Energy, injury and beyond. Br J Pharmacol 171: 1795-1797, 2014.